

# CSAW: A Dynamical Model of Protein Folding

Kerson Huang\*

Physics Department,  
Massachusetts Institute of Technology,  
Cambridge, MA 02139, USA

and

Zhou Pei-Yuan Center for Applied Mathematics,  
Tsinghua University,  
Beijing 100084, China

March 23, 2022

## Abstract

CSAW (conditioned self-avoiding walk) is a model of protein folding that combines the features of SAW (self-avoiding walk) and the Monte-Carlo method. It simulates the Brownian motion of a chain-molecule in the presence of interactions. We begin with a simple model that takes into account the hydrophobic effect and hydrogen bonding. The results show that the hydrophobic effect alone establishes a tertiary structure, which however has strong fluctuations. When hydrogen bonding is added, helical structures emerge, and the tertiary structure becomes more stable. The evolution of the chain exhibits a rapid hydrophobic collapse into a "molten globule", whose slow transition to the final equilibrium state mimics experimental data. The model is designed so that one can add desired features step by step.

## 1 Introduction

We propose a model of protein folding, CSAW (conditioned self-avoiding walk), which is a combination of SAW (self-avoiding walk) and Monte-Carlo. The general idea is that a protein chain in an aqueous solution undergoes Brownian motion due to random impacts from water molecules. At the same time, it is subjects to constraints and organized forces. One the constraint is that residues on the chain cannot occupy the same position. This is taken into account through SAW. Other forces and interactions, such as the hydrophobic effect arising from the water network, and interactions among the residues on the protein chain, are taken into account through a Monte-Carlo procedure.

---

\*Email: kerson@mit.edu

Just as simple random walk simulates the Langevin equation, the present procedure simulates a generalized Langevin equation that describes the protein chain in a native environment.

Our working goal is to begin with a very simple model that nevertheless captures the essence of the protein chain, and add on more realistic features step by step. The starting point is to construct the backbone of the protein molecule as a sequence of connected "cranks" made up of the bonds lying in the amide plane. The orientation of a crank relative to its predecessor is specified by the usual pair of torsional angles. We can then attach extra bonds and side chain as desired, like adding components in an erector set.

As a first attempt, we take the hydrophobic effect into account by assigning each residue with a hydrophobic index 0 or 1, and define a configuration energy that favors the shielding of hydrophobic residues from the environment. This simple models show that the hydrophobic effect alone establishes a tertiary structure, which however has strong fluctuations.

Next, we take into account hydrogen bonding among the residues. To do this, we first attach  $O$  and  $H$  atoms to the cranks, through bonds with the correct lengths and angles. We then introduce an attractive potential between the  $O$  and  $H$  atoms, which depends on their separation and the relative angle of their bonds. The addition leads to the following new phenomena:

- Secondary structure emerges in the form of alpha-helices, and stabilizes the tertiary structure.
- The chain rapidly collapses to an intermediate "molten globule" state, which lasts for a relatively long time before decaying slowly to the native state. The evolution of the radius of gyration agrees qualitatively with experimental observations.

These preliminary results indicate that, compared with molecular dynamics, the CSAW model uses less computer time, and makes the physics more transparent. It merits further examination and development.

This work was first described in lectures given at Tsinghua University in 2005, which were sequels to an earlier lecture series [1]. In that earlier series we developed the view that protein folding should be treated as a stochastic process [2], and CSAW is an implementation of that philosophy.

## 2 Random walk and Brownian motion

Let us review the Brownian motion of a single particle suspended in a medium. Its position  $x(t)$  is a stochastic variable describe by the Langevin equation [3]

$$m\ddot{x} = F(t) - \gamma\dot{x}. \quad (1)$$

The force on the particle by the medium is split into two parts: the damping force  $-\gamma\dot{x}$  and a random component  $F(t)$ , which belongs to a statistical

ensemble with the properties

$$\begin{aligned}\langle F(t) \rangle &= 0, \\ \langle F(t)F(t') \rangle &= c_0 \delta(t - t').\end{aligned}\tag{2}$$

where the brackets  $\langle \rangle$  denote ensemble average. The equation can be readily solved. What we want to emphasize is that It can also be simulated by random walk [4]. Both procedures give rise to diffusion, with diffusion coefficient  $D = \frac{c_0}{2\gamma^2}$ .

In the presence of a regular (non-random) external force  $G(x)$ , the Langevin equation may not be soluble analytically, but we can solve it on a computer via *conditioned random walk*. We first generate a trial step at random, and accept it with a probability according to the Monte-Carlo method, which is usually implemented through the Metropolis algorithm [5]. Let  $E$  be the energy associated with the external force  $G$ , In this case,  $E$  is just the potential energy such that  $G = -\partial E/\partial x$ . Let  $\Delta E$  be the energy change in the proposed update. The algorithm is as follows:

- If  $\Delta E \leq 0$ , accept the proposed update;
- If  $\Delta E > 0$ , accept the proposed update with probability  $\exp(-\Delta E/k_B T)$ .

The last condition simulates thermal fluctuations. After a sufficiently large number of updates, the sequence of state generated will yield a Maxwell-Boltzmann distribution with potential energy  $E$ .

The conditioned random walk may be described in terms of the Langevin equation as follows:

$$m\ddot{x} = \underbrace{[F(t) - \gamma\dot{x}]}_{\text{Treat via random walk}} + \underbrace{G(x)}_{\text{Treat via Monte-Carlo}}.\tag{3}$$

### 3 SAW and CSAW: Brownian motion of a chain molecule

A protein molecule in its denatured (unfolded) state can be simulated by a random coil. That is, it is a long chain undergoing Brownian motion in a medium. The time development is a sequence of random chain configurations, with the restriction that two different residues cannot overlap each other. An instantaneous configuration is therefore a *self-avoiding walk* (SAW) — a random walk that never crosses itself.

For illustration, we can generate a SAW with hard-sphere exclusion on a computer, as follows:

- Specify a step size, a starting position, and a radius of exclusion around an occupied position.
- \* Make a random step of the given magnitude and arbitrary direction.

- If the step does not overlap any of the previous positions, accept it, otherwise go to \*.

By repeating the procedure  $N$  times, we generate a SAW representing the instantaneous configuration of an  $N$ -chain.

A uniform ensemble of chains can be generated by the pivoting method [6] [7]:

- Start with an initial SAW chain. Take one end as a fixed origin.
- \*\* Choose a random position on the chain. Rotate the end portion of the chain about this position, through a randomly chosen rotation.
- If the resulting chain does not overlap the original chain, accept it as an update, otherwise go to \*\*.

The rotation is a random operation making use of the allowed degrees freedom of the chain. In a protein chain, this consists of rotation the two torsion angles.

After a sufficient number of warm-ups, the procedure generates a sequence of SAW chains belonging to a statistical ensemble that is ergodic and uniform, *i.e.*, it includes all possible SAW's with equal probability. The sequence of updates may be taken as a simulation of the approach to thermal equilibrium with the environment.

Formally speaking, we are simulating the solution of a generalized Langevin equation of the form [8]

$$m_k \ddot{\mathbf{x}}_k = \mathbf{F}_k(t) - \gamma_k \dot{\mathbf{x}}_k + \mathbf{U}_k(\mathbf{x}_1 \cdots \mathbf{x}_N), \quad (k = 1 \cdots N) \quad (4)$$

where the subscript  $k = 1 \cdots N$  labels the residue along the chain. The term  $\mathbf{U}_k$  includes the forces that maintain a fixed distance between successive residues, and prohibit the residues from overlapping one another. Other interactions are neglected when the chain is in an unfolded state. The SAW algorithm is a special case of a Monte-Carlo procedure in which the energy change is either 0 (if there are no overlaps), or  $\infty$  (if there is an overlap).

The protein begins to fold when placed in an aqueous solution, because of the hydrophobic effect. To model the process, we must include the interactions among residues, as well as their interactions with the medium. The generalized Langevin equation still has the form (4), with added interactions:

$$m_k \ddot{\mathbf{x}}_k = \underbrace{(\mathbf{F}_k - \gamma_k \dot{\mathbf{x}}_k + \mathbf{U}_k)}_{\text{Treat via SAW}} + \underbrace{\mathbf{G}_k}_{\text{Treat via Monte-Carlo}}. \quad (5)$$

As indicated on the right side of the equation, we simulate this equation via CSAW (*conditioned self-avoiding walk*). The interaction forces  $\mathbf{G}_k$ , which was neglected in the unfolded case, is now taken into account through Monte-Carlo.

To learn how to include the forces  $\mathbf{G}_k$ , we first consider simple examples, and then try to build a more realistic model step by step.

## 4 The action of water

The hydrophobic effect drives a protein chain to its folded configuration, and maintains it in that configuration. The effect has its origin in the hydrogen bonding between water molecules results in a fluctuating water network with a characteristic time of  $10^{-12}\text{s}$ .

The residues in a protein molecule can be chosen from a pool of 20 amino acids, differing from each other only in the structure of the side chain, which can be polar (possessing an electric dipole moment) or nonpolar. The polar ones can form hydrogen bonds with water, and are said to be *hydrophilic*. The nonpolar ones cannot form hydrogen bonds, and are said to be *hydrophobic*. The presence of the latter robs water molecules of the opportunity to form hydrogen bonds, and disrupts the water network. It induces an effective pressure from the water network, to have the hydrophobic residues shielded by hydrophilic ones, to prevent them from coming into contact with water. The folded state of the protein is determined by how this could be done with least cost to everyone involved.

While the side chains may be hydrophilic or hydrophobic, the backbone is hydrophilic. Frustration arises when one attempts to bury the hydrophobic residues in the interior of the molecule, because the part of backbone that gets buried loses contact with water. The frustration is resolved by the formation of secondary structures,  $\alpha$ -helices and  $\beta$ -strands, in which hydrogen bonding occurs among different residues. Thus, the tertiary structure and the secondary structure are coupled to each other.

The action of water on the protein molecule can be divided into 3 aspects:

- Thermal motion of water molecules induce Brownian motion of the protein chain, folded or not. This is the thermalizing interaction.
- The water network applies pressure to the protein, squeezing it into the folded state and maintain it in that state. This is the hydrophobic effect.
- The water network has vibrational modes in a wide range of frequencies. The low-frequency modes can resonate with low normal modes of the protein molecule. These are associated with shape oscillations of the protein, and the input energy is transferred to modes of higher frequency, initiating an energy cascade down the length scales of the protein molecule. The significance of this interaction was explored [9], but remains to be understood.

The resonance between water and protein can be illustrated in more detail. Fig.1 shows both the spectrum of water [10] and the spectrum of a small protein [11], both based on calculations. We can see there is a prominent peak in both spectrum at a frequency of about  $100\text{ cm}^{-1}$ . Resonant oscillation between protein and water can occur at this peak. In water, this mode corresponds to a collective motion of the  $O$  atoms in the network, while In the protein it corresponds to a shape oscillation.

## 5 First model

In the first model, we take the residues as impenetrable hard sphere, with diameter equal to the distance between successive residues. The hydrophobic effect is taken into account using a simple "PH model" [12] in which the residues are either polar (P) or hydrophobic (H).

- The centers of the hard spheres (corresponding to  $C_\alpha$  atoms,) are connected by "cranks" made up of bonds. to be described in detail later. The relative orientation of two successive cranks is specified by the two torsional angles  $\psi, \phi$ . With one end fixed, the degrees of freedom of an  $N$ -chain are the  $N - 1$  sets of angles  $\{\psi_j, \phi_j\}$  ( $j = 2, \dots, N$ ).
- The energy  $E$  of a configuration is given by

$$E = -gK,$$

$$K = \text{Contact number of hydrophobic residues.} \quad (6)$$

A residue's contact number is the number of other residues in contact with it, *not counting those lying next to it along the chain*. Two residues are in contact when their centers are separated by less than a set fraction (say, .1.2) of the residue diameter.

- When two H are in contact, the total contact number increases by 2. This induces an attractive force between H residues.

Remarks:

- The denatured chain in a non-aqueous solution corresponds to  $g = 0$ .
- Only  $E/(k_B T)$  appears in the Metropolis algorithm, Thus only the combination  $g/(k_B T)$  matters.

## 6 Example in 2D

We first illustrate the model in a simple setting to show that it has merit. Here, the monomer on the chain are connected by straight bonds.

Consider a chain of 7 circular monomers in 2D continuous space, with only one H. The configuration for maximal shielding of H from the medium is a hexagonal close pack with H at the center. We shall show that CSAW reproduces this result.

Take the hard sphere diameter to be 1. The H monomer is considered shielded by another monomer, if the distance to the latter is less than 1.2. The maximum number of nearest neighbors is 4, as illustrated in the Fig.2.

Fig.3 displays the evolution of the 2D chain in different runs, with H (the black dot) placed at different positions on the chain. The numerals under each configuration are the Monte-Carlo steps. We see that all runs tend to the hexagonal close pack, thus illustrating "convergent evolution". The lowest panels shows the evolution of the rms radius.

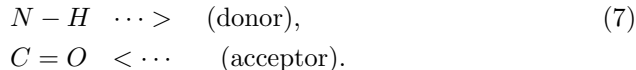
Bonds	(A)	Angles	(°)
$C_\alpha - C$	1.53	$C_\alpha - C - O$	121
$C - O$	1.25	$C_\alpha - C - N$	114
$C - N$	1.32	$O - C - N$	125
$N - H$	1.00	$C - N - H$	123
$N - C_\alpha$	1.41	$C - N - C_\alpha$	123

Table 1: Bond lengths and angles in the crank

## 7 The protein chain

We review salient properties of the protein chain, with a view to design a model that can be incrementally improved as work progresses.

Fig.4 shows a schematic representation of the protein chain. The center of each residue is a carbon atom denoted  $C_\alpha$ . Of particular relevance is whether a molecular group in a residue is polar (P, or hydrophilic) or nonpolar (H, or hydrophobic). The backbone contains polar subunits  $N - H$  and  $C = O$  that can participate in hydrogen bonding. The former wants to donate an  $H$  atom, while the latter seeks an  $H$  atom:



They cannot bond with each other, however, because the bond length is not correct. They may bond with water molecules in the medium, or with other residues. The latter possibility leads to the secondary structures in the protein chain. The side chains  $R$  attached to a  $C_\alpha$  atom, may be P or H, and this determines whether the residue is taken to be P or H.

Geometrically, the  $C_\alpha$  atom sits at the center of a tetrahedron form by the four atoms NRHC, as shown in Fig.5. The  $H$  atom here does not participate in hydrogen bonding, because the  $C_\alpha - H$  group is nonpolar.

The connecting group between two successive  $C_\alpha$ 's is made up of four atoms  $OCNH$ , which lie in a single plane, the *amide plane*. The bonds in  $-C - N-$  are arranged in the shape of a "crank", as illustrated in the upper panel of Fig.6. The bond lengths and angles of the crank are given in Table(1). As indicated in the lower panel of Fig.6, the backbone of the protein is a sequence of cranks joined at a tetrahedral angle  $\cos^{-1}(-1/3) \approx 109.5^\circ$ .

## 8 Torsional angles

The relative orientation of two successive cranks is specified by two torsional angles  $\{\psi, \phi\}$ . In Fig.6, the angles associated with crank 2 are defined as follows:

$$\begin{aligned}\psi &= \text{Rotation angle of } N_2 \text{ about axis } C_{\alpha 2} \rightarrow C_2. \\ \phi &= \text{Rotation angle of } C_1 \text{ about axis } C_{\alpha 2} \rightarrow N_1, \\ &= \text{Rotation angle of } C_2 \text{ about axis } N_1 \rightarrow C_{\alpha 2}.\end{aligned}\tag{8}$$

where the subscripts 1,2 refer respectively the atoms in crank 1 and crank 2.

In the flat configuration we have  $\psi = \phi = \pi$  by definition. This configuration, however, cannot be realized, because of a collision between  $H$  and  $O$  in successive residues. Because of such exclusions, the angles are restricted to allowed regions, as displayed in the Ramachandran plots shown in Fig.7.

A secondary structure is formed by a sequence of cranks all having the same torsional angles. The three allowed areas on the Ramachandran plot are associated respectively with the right-handed  $\alpha$ -helix, the  $\beta$ -strand, and the left-handed  $\alpha$ -helix. Examples are shown in Fig.8.

A right-handed  $\alpha$ -helix is formed by setting all angles to the values  $\psi \approx -50^\circ$ ,  $\phi \approx -60^\circ$ . The hydrogen bonding has the pattern

$$\begin{aligned}(C = O)_1 \cdots (H - N)_4, \\ (C = O)_2 \cdots (H - N)_5.\end{aligned}\tag{9}$$

*etc.*, where the subscripts labels the residue. In a  $\beta$ -strand, the angles have the approximate values  $\psi \approx \phi \approx -150^\circ$ . Such strands are matted together to form a  $\beta$ -sheet, through the formation of hydrogen bonds.

The secondary structure are unstable in the denatured state, because the energy advantage in hydrogen bonding does not overcome the desire for more entropy. In this state, hydrogen bonding switches from residue to residue, or to water. The characteristic time should be  $10^{-12}$ s, if we can take the water network as reference.

## 9 Hydrophobic collapse

In this exercise, we leave out all interactions except the hydrophobic effect. The residues are taken be hard spheres with diameter equal to the distance to the next neighbor, connected to each other by cranks. Thus, we have a chain of beads that can twist and turn through changes in the torsional angles. Some computer-generated chains are shown in Fig.9.

Fig.10 shows the evolution of a chain of 10 cranks, with only one H, in three separate runs with different placements of the H. After about 1000 Monte-Carlo steps, the chain collapses to compact configurations with the H surrounded. A hexagonal geometry can be discerned. although there is considerable fluctuation in the shape. Close-packing of free spheres in 3D will lead to hexagonal or cubic



close pack, in which each sphere touches 12 nearest neighbors [13]. This cannot be realized here, because of the intervention of the connecting cranks.

Next, we consider 20 cranks with two H, and the results are displayed in Fig.11. We can see that the two H are attracted to each other, and the other residues try to a close pack with the pair in the center.

Finally we consider a chain of 30 cranks, with 1/3 of the residues being H. This is the approximate ratio in a real protein. As shown in Fig.12, the chain settles into a tertiary structure resembling a three-leaf clover. The lowest panel of the figure shows backbone images of the tertiary structure by RasMol [14]. The local structure fluctuates considerably, but the general topology is unmistakable. We conclude that hydrophobic forces alone leads to a well-defined tertiary structure in the final state.

## 10 Hydrogen bonding

We now improve the model by taking into account hydrogen bonding. First we must attach the  $O$  and  $N$  atoms to the crank, so that there are now  $C = O$  and  $N - H$  bonds in the amide plane. A hydrogen bond is formed between  $O$  and  $H$  from different residues, when

- the distance between  $O$  and  $H$  is 2 Å, within given tolerance;
- The bonds  $C = O$  and  $N - H$  are antiparallel, within given tolerance.

When these conditions are fulfilled, the energy of the configuration is lowered by the bond energy [15]. The formation of such a bond is illustrated in Fig.13. The residues are still either hydrophobic (H) or hydrophilic (P); but they are no longer treated as hard spheres. The self-avoidance condition now takes into account collisions among the  $H$  and  $O$  atoms on the newly added bonds.

The energy of a configuration that replaces (6) is

$$\begin{aligned} E &= -g_1 K_1 - g_2 K_2, \\ K_1 &= \text{No. of nearest neighbors of hydrophobic residues,} \\ K_2 &= \text{No. of hydrogen bonds.} \end{aligned} \tag{10}$$

In the Monte-Carlo update only the combinations  $g_1/k_B T$  and  $g_2/k_B T$  are relevant. In practice, we set  $k_B T = 1$  and treat  $g_1$  and  $g_2$  as adjustable parameters. At this stage of modeling, we are not ready to calibrate these parameters through comparison with experiments.

There is an implicit assumption about hydrogen bonding, namely, atoms on the side chains can bond with water, while atoms on the backbone can only bond with each other. This is reflected in the division of the energy into the  $g_1$  and  $g_2$  terms. The  $g_1$  term simulates the hydrophobic effect arising from bonding between side chains and water. The  $g_2$  term, on the other hand, counts only the hydrogen bond among the residues themselves. This division correspond to experimental fact, but by assuming it we have introduced a bias

into the model. We think it does not bias the results, but only further study can confirm this.

As a test of the hydrogen-bonding interaction, we turn off the hydrophobic interaction by setting  $g_1 = 0$ . With  $n = 30$ ,  $g_2 = 1$ , an  $\alpha$ -helix emerges after 1000 Monte-Carlo steps, as depicted in Fig.14.

## 11 Formation of secondary structure

To illustrate the formation of secondary structure, we consider a chain of 30 residues with 10 hydrophobic residues, at positions 1,3,6,7,10,16,20,23,26,29. We set  $g_1 = 10$ ,  $g_2 = 8$ .

The evolution of the radius of gyration is shown in Fig.15. After a rapid collapse, there is a long stretch that we identify with the molten globule state, which eventually makes a transition to the native state. The change in radius is relatively small, and discernible only in a magnified view. The slow transition to the native state mimics experimental data from the folding of apomyoglobin [16], as displayed in the lowest panel of the figure.

It is interesting that, during the fast collapse, the radius first decreases, and then expands before resuming the collapse. This could be an example of the "Reynolds dilatancy" observed in granular flow [17].

Images of the chain are shown in Fig.16. The ones at 2000 and 40000 steps correspond to the molten globule, and the last one at 60000 corresponds to (as far as we can tell) the native state. The all show two short helices connected by a loop, with no significant differences to the eye. That is, the molten globule already possesses the architecture and the compactness of the native state.

Other runs with the same parameters do not yield the same transition points between the molten globule and the native state. This suggests that the transition is initiated by nucleation, as in a first-order phase transition. A more careful statistical study is in progress.

## 12 Conclusion

The advantage of CSAW is that it is simple in conception, flexible in design, and fast in execution. We can start with a backbone made up of a sequence of bare cranks, and add components step by step. At each stage we can see the difference made, thereby gain insight into the physical roles played by different elements in the chain. Our eventual goal, which does not appear to be extravagant, is to model a protein molecule with full side chains.

I thank Zuoqiang Shi, physics graduate student at Tsinghua University, for helping me with the computations on the secondary structures.

## References

- [1] K. Huang, *Lectures on Statistical Physics and Protein Folding* (World Scientific Publishing, Singapore, 2005), hereafter referred to as *Lectures*.
- [2] K. Huang, *Introduction to Statistical Physics* (Taylor & Francis, London, 2001), hereafter referred to as *Statistical Physics*.
- [3] *Lectures*, Chap.10 and Appendix.
- [4] *Lectures*, Chap.9; *Statistical Physics*, p.72.
- [5] *Statistical Physics*, Sec.18.9.
- [6] B. Li, N. Madras, and A.D. Sokal, *J. Stat. Phys.* **80**, 661 (1995).
- [7] T. Kennedy, *J. Stat. Phys.* **106**, 407 (2002).
- [8] V.N. Prokrovskii, *The Mesoscopic Theory of Polymer Dynamics* (Kluwer Academic Publishers, Dordrecht, 2000).
- [9] *Lectures*, Chap.16 and Appendix.
- [10] S. Saito, I. Ohmine, *J. Chem. Phys.* **102**, 3566-3579 (1995).
- [11] N. Go, T. Noguti, T. Nishikawa, *Proc. Nat. Acad. Sci., USA*, **80**, 3696-3700 (1983).
- [12] H. Li, C. Tang, N.N. Wingren, *Proc. Nat. Acad. Sci., USA*, **95**, 4987-4990 (1998).
- [13] J. H. Conway and N.J.A. Sloane, *Sphere Packings, Lattices, and Groups*, 2nd ed. (Springer-Verlag, New York, 1993).
- [14] RasMol homepage: <http://www.umass.edu/microbio/resmol/>
- [15] A. V. Smith and C.K. Hall, *Proteins*, **44**, 344-360 (2001) uses a similar model of hydrogen bonds in a molecular-dynamics computation.
- [16] T. Uzawa, S. Akiyama, T. Kimura, S. Takahashi, K. Ishimori, I. Morishima, T. Fujisawa, *Proc. Nat. Acad. Sci., USA*, **101**, 1171-1176 (2004).
- [17] O. Reynolds, "On the dilatancy of media composed of rigid particles in contact. With experimental illustrations", *Philosophical Magazine* (December, 1885).

## Figure Captions

Fig.1. Calculated spectrum of normal modes of liquid water network (upper panel) and that of a protein molecule (lower panel). They resonate at a frequency of about  $100\text{ cm}^{-1}$ .

Fig.2. The hydrophobic residue on the chain is represented by the dark circle. It can have a maximum of 4 nearest neighbors, not counting those on the chain.

Fig.3. Upper panels: Evolution of the chain, with the hydrophobic residue shown as a black dot. Regardless of its placement, the chain tends to a hexagonal close pack, with hydrophobic residue in the center. Lowest panel: Evolution of the rms radius, showing hydrophobic collapse and steady state equilibrium.

Fig.4. Schematic representation of the protein chain.

Fig.5. Tetrahedron with the  $C_\alpha$  atom at the center.

Fig.6. Upper panel: Two successive  $C_\alpha$  atoms are joined by chemical bonds in the shape of a "crank". Side chains and H atoms attached to  $C_\alpha$  have been omitted for clarity. Lower panel: The protein backbone is a sequence of cranks joined at a fixed angle. The orientation of the plane of one crank, relative to the preceding one, are specified by two torsional angles  $\phi, \varphi$ .

Fig.7. Ramachandran plots of allowed regions for the torsional angles.

Fig.8. Examples of secondary structure. Hydrogen bonds are indicated by dotted lines.

Fig.9. Examples of a chain of hard-spheres connected by cranks.

Fig.10. Chain of 10 cranks with 1 H, which is represented by the solid circle. Three different runs are shown, with different placements of H. All result in the H being surrounded by other residues in an attempt to achieve hexagonal or cubic close packing. For clarity, we hide the cranks, and connect the  $C_\alpha$  atoms by straight bonds.

Fig.11. The hydrophobic effect induces an effective attraction between to hydrophobic residues.

Fig.12. Chain of 30 cranks, with 1/3 of the residues being H. Lowest panel displays RasMol backbone images, at the Monte-Carlo steps as labeled.

Fig.13. A hydrogen bond is formed when the distance between  $O$  and  $H$  lie within given limits, and the bonds they belong to are antiparallel within given tolerance.

Fig.14. Testing the hydrogen-bonding interaction with  $g_1 = 0$  (no hydrophobic effect). An  $\alpha$ -helix emerges after 1000 Monte-Carlo steps, as shown here in backbone and spacfill representations by RasMol.

Fig.15. The strong radius fluctuation during the initial collapse suggests "Reynolds dilatancy", a phenomenon in granular flow. After the collapse, the radius remains constant for a relatively long time. This corresponds to the "molten globule" stage, which slowly decays to the native state, with a small decrease of the radius. For comparison, the lowest panel shows experimental data from the folding of apomyoglobin.

Fig.16. RasMol backbone images of the chain. There are two short helices connected by a loop. The first two images corresponds to the molten globule

state, and the last corresponds to the native state.

This figure "fig1.jpg" is available in "jpg" format from:

<http://arxiv.org/ps/cond-mat/0601244v1>

This figure "fig2.jpg" is available in "jpg" format from:

<http://arxiv.org/ps/cond-mat/0601244v1>

This figure "fig3.jpg" is available in "jpg" format from:

<http://arxiv.org/ps/cond-mat/0601244v1>



This figure "fig4.jpg" is available in "jpg" format from:

<http://arxiv.org/ps/cond-mat/0601244v1>

This figure "fig5.jpg" is available in "jpg" format from:

<http://arxiv.org/ps/cond-mat/0601244v1>

This figure "fig6.jpg" is available in "jpg" format from:

<http://arxiv.org/ps/cond-mat/0601244v1>

This figure "fig7.jpg" is available in "jpg" format from:

<http://arxiv.org/ps/cond-mat/0601244v1>

This figure "fig8.jpg" is available in "jpg" format from:

<http://arxiv.org/ps/cond-mat/0601244v1>

This figure "fig9.jpg" is available in "jpg" format from:

<http://arxiv.org/ps/cond-mat/0601244v1>

This figure "fig10.jpg" is available in "jpg" format from:

<http://arxiv.org/ps/cond-mat/0601244v1>

This figure "fig11.jpg" is available in "jpg" format from:

<http://arxiv.org/ps/cond-mat/0601244v1>



This figure "fig12.jpg" is available in "jpg" format from:

<http://arxiv.org/ps/cond-mat/0601244v1>

This figure "fig13.jpg" is available in "jpg" format from:

<http://arxiv.org/ps/cond-mat/0601244v1>

This figure "fig14.jpg" is available in "jpg" format from:

<http://arxiv.org/ps/cond-mat/0601244v1>

This figure "fig15.jpg" is available in "jpg" format from:

<http://arxiv.org/ps/cond-mat/0601244v1>

This figure "fig16.jpg" is available in "jpg" format from:

<http://arxiv.org/ps/cond-mat/0601244v1>